

Design for Robust and Efficient Neuromorphic Photonic Accelerator

Samarth Aggarwal
Department of Materials
Univeristy of Oxford
Oxford, United Kingdom

Bowei Dong
Department of Materials
Univeristy of Oxford
Oxford, United Kingdom

June Sang Lee
Department of Materials
Univeristy of Oxford
Oxford, United Kingdom

Mengyun Wang
Department of Materials
Univeristy of Oxford
Oxford, United Kingdom

Andrew Katumba
Ghent university/imenc
Ghent, Belgium

Peter Bienstmana
Ghent university/imenc
Ghent, Belgium

Harish Bhaskaran
Department of Materials
Univeristy of Oxford
Oxford, United Kingdom
harish.bhaskaran@materials.
ox.ac.uk

Abstract—In this work, we propose a novel architecture for building a robust integrated photonic neuromorphic accelerator based on a crossbar array design. Our architecture is based on an asymmetric multimode Y-coupler. A Y-coupler has the inherent benefit of high fabrication tolerance and broad optical bandwidth. From simulations, we show that our proposed Y-coupler has high coupling efficiency. Using modal decomposition analysis of our coupler, we numerically estimate the energy efficiency performance of a large-scale photonic network and show a 10% improvement in energy efficiency for large-scale photonic networks with high fabrication tolerance and broadband application and a small footprint.

Keywords—*Neuromorphic Computing; Integrated Photonics; Photonic Architecture; Multimode System*

I. INTRODUCTION

The increase in demand for computing power has resulted in a data transfer bottleneck known as the von-Neumann bottleneck. Therefore, various specialized hardware for in-memory computing has been proposed. With the slowing down of Moore's law, optical solutions for neuromorphic computing have been demonstrated as an alternative to electronics. Optical solutions despite their larger size, have an inherent advantage of higher processing throughput using various multiplexing schemes like wavelength and polarization therefore resulting in a larger computation density. Recently, in integrated photonic, an architecture using waveguide and phase change materials-based memory has been shown to form an excellent way of performing in-memory multiply and accumulate (MAC) operations¹. Such architectures have been shown to perform computationally intensive tasks like convolution for pattern and image recognition^{2,3}. However, the scalability of such networks is limited due to high optical losses.

A crossbar array architecture has multiple nodes comprising of a number of splitters and couplers. Unlike electronics combining optical power is not as straightforward as adding two voltage or current. A coupler based on a single mode Y-splitter (-3dB coupler) results in a 50% loss of optical power at each junction. This limits the number of nodes in a photonic network and therefore limits the scalability of photonic networks. The optical power of the first input node drops exponentially as it passes through each node. The issue of unequal power loss at each node can be resolved using directional couplers and distributing the coupling losses equally amongst the coupling nodes, as shown in our previous

work²; however, the overall optical loss of the system remains the same using both approaches.

Another drawback of using directional couplers is their sensitivity to small fabrication errors, high sensitivity to wavelength⁴ and a large footprint. Other passive approaches of combing optical signals using wavelength division multiplexing (WDM) using ring resonators⁵ have similar issues to a directional coupler. They also have high sensitivity to fabrication errors and limited bandwidth. As we will show further, for foundry fabricated devices, there is a mismatch in the power coupling ratio of different optical signals due to fabrication variations across the wafer. A Y-coupler would thus yield a reliable and robust large-scale optical design with a smaller footprint.

A multimode coupler was proposed for reservoir computing applications with a high number of nodes, as in neuromorphic computing hardware⁶. The coupling efficiency of such Y-couplers can be improved by considering asymmetric coupler design. Work on optical fibers has also demonstrated the advantages of using asymmetric multimode fibers for efficient signal coupling in linear data bus⁷. In this work, we design an integrated photonic coupler that uses principles of both multimode and asymmetric couplers. We perform modal decomposition simulations and, using a scattering matrix approach, estimate the coupling efficiency of an asymmetric multimode Y-coupler. We then compare the performance of our device with a directional coupler and a single mode Y-coupler and demonstrate a superior broadband performance with lower sensitivity to fabrication variations.

II. DEVICE DESIGN

Our design is based on a standard 220 nm silicon-on-insulator (SOI) platform at 1550 nm wavelength. As shown in the device schematic in Figure 1, our coupler has three ports: a single mode Port 1 (Input Signal), multimode Port 2 (Input Bus) and multimode Port 3 (Output Bus). At each node N_i , Transverse Electric (TE_0) signal with the wavelength λ_i is injected at port 1. A unique wavelength at each node ensures no interference between input signals. This interference issue can also be avoided by use of an incoherent light source as an input signal. The Input Signal is coupled to the Input Bus from port 2 to obtain an Output at port 3. The input power from a single mode port 1 is converted to higher order modes at the output of port 3.

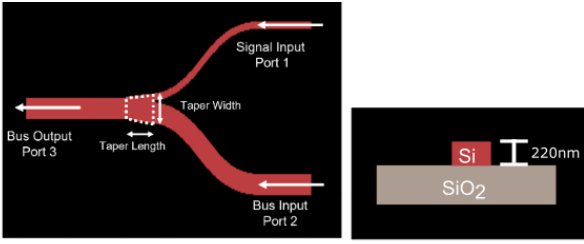


Figure 1 Schematic diagram of the proposed asymmetric coupler with three ports. A single mode signal is coupled into the Bus input (port 2), resulting in a multimode output at Bus Output (Port 3).

To achieve high coupling efficiency, the device is designed to have a high transmission for all higher order modes. To achieve high average transmission of all incident modes, the taper length of the coupler has to be optimized to balance two conflicting effects⁶. Increasing the taper length decreases the scattering losses of the supermodes in the taper section. However, increasing the taper length decreases the mode conversion efficiency of higher order supermodes in the taper to lower order modes at the output. Therefore using the particle swarm optimization method in Lumerical FDTD, we optimize the geometry of our asymmetric Y coupler for average transmission, by varying the waveguide width of the input bus waveguide, taper width and taper length. The dimensions of the input and output multimode waveguides are kept equal to simplify the simulation optimization. The final dimensions of our coupler are shown in Table 1.

Table 1: Summarizing the design parameters of the proposed asymmetric directional coupler obtained from Particle Swarm optimization in Lumerical FDTD simulations.

Device Parameters		Unit
Bus Input Width	1460	nm
Signal Input Width	500	nm
Taper Width	1960	nm
Taper Length	3870	nm
Bend angle	5	degree

It is worth noting, the small footprint of our device as compared to a directional coupler. Our device has a footprint of less than $5 \mu\text{m}$ in total length as compared to a directional coupler where the coupling lengths can vary from $10\text{-}30 \mu\text{m}$ for a similar 220nm SOI platform. This results in a smaller overall computing unit cell and hence can result in over 5 times improvement in compute density reported in our previous work².

We observe that five modes are supported in the bus waveguide, with the first four modes strongly guided and a fifth weakly guided mode. In Figures 2 (a-f), we plot the E-field profile of various modes through port 2 and 3 of our coupler device. Furthermore, using simulations, we calculate the transmission of various modes from both the signal input and bus input waveguides and calculate the modal power distribution, as shown in Table 2 and Table 3. The modal power distribution can be represented as transfer matrix T_1 and T_2 respectively.

In a multimode system different modes have different group velocities in the waveguide. This results in relative delay between signals of different modes and thereby calculating the transmission loss a complex function and difficult to calculate analytically. However, we can use the power distribution transfer matrix (T_1 and T_2) to calculate the approximate power drop with increasing number of nodes.

Table 2: Modal power distribution at Output Bus (Port 3) when single mode TE_0 light is injected at Signal Input port (Port 1), with a net transmission of 97.5%.

Modal Distribution	Signal Input
TE0	0.101
TE1	0.342
TE2	0.352
TE3	0.148
TE4	0.030
Net Transmission	0.975

Table 3: Modal power distribution at Output Bus (Port 3) when various mode $\text{TE}_0\text{-TE}_4$ are injected at Bus Input port (Port 2), with a complex power distribution across various modes.

Input ->	TE0	TE1	TE2	TE3	TE4
TE0	0.7769	0.0474	0.0668	0.0027	0.0015
TE1	0.0534	0.4398	0.1086	0.0450	0.0020
TE2	0.1175	0.1144	0.3862	0.0056	0.0005
TE3	0.0393	0.3678	0.3610	0.0394	0.0058
TE4	0.0038	0.0037	0.0318	0.7309	0.0958
Net Transmission	0.9908	0.9730	0.9543	0.8237	0.1057

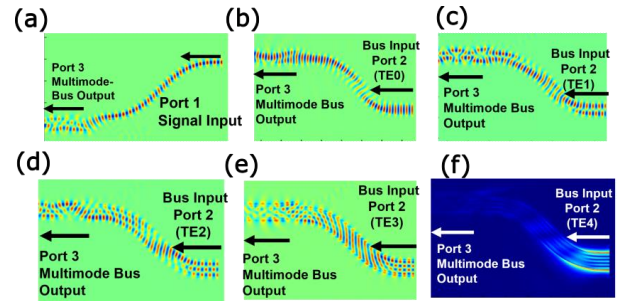


Figure 2: (a) E_y -field profile when TE_0 signal is injected at port 1.(b)-(e) E_y -field profile when $\text{TE}_0\text{--TE}_3$ input is injected at Bus Input (port 2). (f) E-field magnitude profile when weakly supported TE_4 input is injected at Bus Input (port 2).

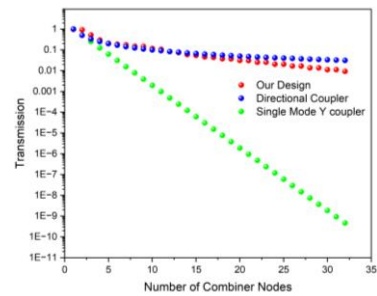


Figure 3: Comparison of performance of our device as compared to a directional coupler and single mode Y-coupler with increasing number of coupler nodes.

The approximate power distribution O_M , after M nodes can be written analytically as :

$$O_M = (T_2)^{M-1} \times T_1$$

To account for the difference in group velocity due to multimode system, we calculate the scattering matrix of our device for various incident modes using Lumerical Interconnect. We calculate the transmission loss of our device for the increasing number of nodes. In Figure 3, we compare the performance of our device with a directional coupler and single mode Y-coupler. Assuming low insertion loss for a directional coupler, the transmission for a directional coupler is plotted as $1/M$ for M nodes in the network. As expected, the transmission of an ideal single mode 3dB Y-coupler drops exponentially ($1/2^M$) for an increasing number of nodes, while the transmission loss of our device is comparable to that of a directional coupler.

III. SYSTEM LEVEL SIMULATIONS

Having shown the higher performance of a single device in terms of optical loss as compared to a single mode Y splitter, we further construct a large optical crossbar array network and test the overall system loss and broadband optical performance of our device. Using Lumerical Interconnect simulations, we find a minimum improvement of 10% (Figure 4) for larger networks, while more than 50% improvement for smaller networks. As the number of nodes are increased more optical power is lost in the system as explained above, thereby explaining the reason for such variations in efficiency.

Further, we carry out system-level bandwidth performance simulations by varying the wavelength of the input signal. As shown in Figure 5, there is no significant change in performance from the wavelength of 1500-1600 nm.

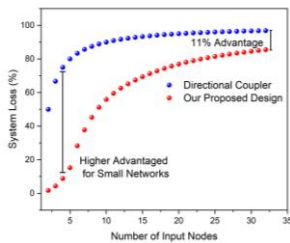


Figure 4: Net System Loss (%) comparison of our device with increasing number of nodes

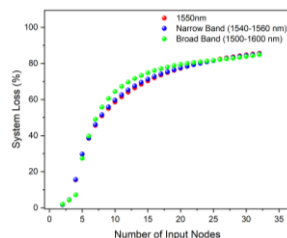


Figure 5: Broadband performance of our device with increasing number of nodes. For wavelengths at 1500-1600nm, system losses are similar to that of single wavelengths.

To test the effect of using a multimode device on the loss of computational bandwidth, we performed bandwidth calculations in Interconnect. To set up the simulation, we use a single source laser and modulate the input optical signal with a randomly generated signal. The output of the optical network is connected to p-i-n junction photodetector. As shown by the eye diagram in Figure 6, there is no loss in computational bandwidth due to multimodal operation for a 32-node network with modulation up to 25 GHz with a very low bit error rate. Therefore using a design based on a multimode waveguide has no effect on data processing speeds.

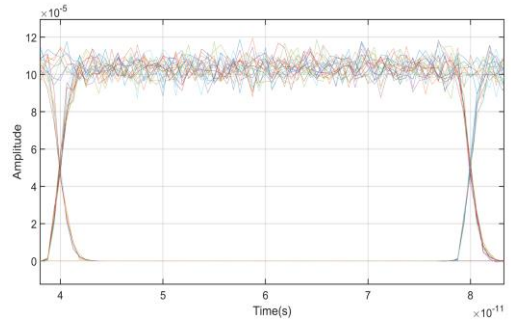


Figure 6: Eye Diagram for 32 node photonic network using our coupler design with a 10mW input signal modulated at 25 GHz, showing negligible bit error rate.

IV. FABRICATION TOLERANCE COMPARISON

In this section, we discuss the advantages of our proposed network using an asymmetric Y-coupler as compared to designs based on directional couplers and WDM using ring resonators.

For design using directional couplers, varying the coupling length of the device results in a different power coupled into the drop port. A small variation in coupling gap or waveguide

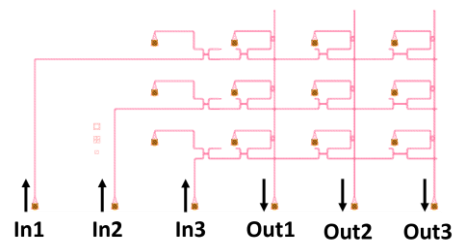


Figure 7 Schematic of a 3x3 photonic network with WDM using ring resonator fabricated in IMEC foundry.

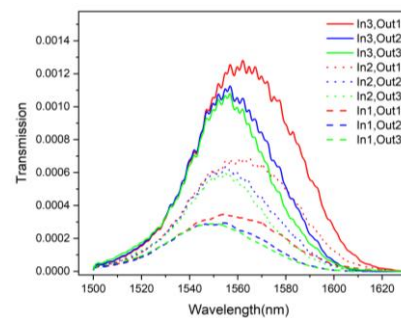


Figure 8 : Variation in coupling power for a 3x3 photonic network based on directional coupler due to fabrication variation.

width from variation in fabrication related tolerances can result in a huge difference in the coupling coefficients of two coupled waveguides. A small 3x3 optical network based on our crossbar array structure (Figure 7), as explained in our previous work², was fabricated in a foundry (IMEC). For a small device, we observe variation in the splitting of power from directional couplers due to fabrication variations across the wafer, Figure 8.

Next, we move our focus onto the design strategy of using WDM with ring resonators to couple power. As shown in Figure 9, for the devices fabricated in a foundry, there is a

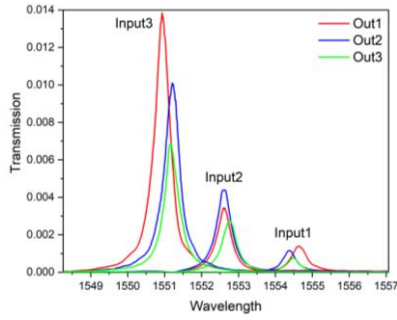


Figure 9 : Variation in coupling power for a 3×3 photonic network based on ring resonator due to fabrication variation and resonance wavelength.

variation in the resonance peaks resulting in the unequal coupling of optical power at each node. This shift in resonance can be corrected using active tuning methods such as microheaters, thus adding to the power budget of the network.

Having discussed the limitations of other photonic network architectures, we test the effect of fabrication variation on the performance of our device. The source of error in fabrication is due to etching depth variation over a wafer and waveguide widths due to lithography variation. Therefore in our simulation, we vary the etching height and waveguide widths to account for fabrication variations. Assuming a 10% deviation in fabrication process, we perform simulations to test the performance of our proposed device. As shown in Figure 10-11, the change in parameters has a limited effect on the performance of our device. These results are important for building a large, robust optical network.

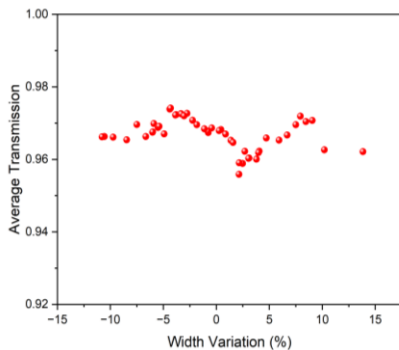


Figure 10 : Effect of waveguide width variation due to fabrication variations on average transmission of our device.

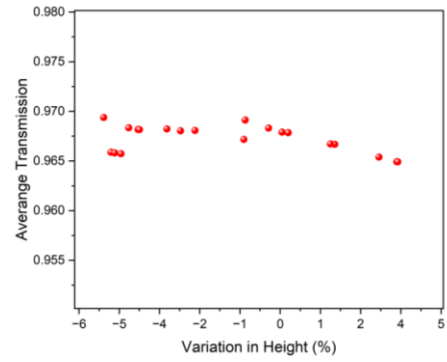


Figure 11: Effect of waveguide thickness due to fabrication variations on average transmission of our device.

V. CONCLUSIONS

In this work, we have proposed a novel photonic architecture using an asymmetric multimode Y-coupler for a neuromorphic computing accelerator. This design has a high optical bandwidth with a small footprint and high tolerance to fabrication errors. For small photonic hardware, our proposed design has 50% better efficiency in terms of optical loss and for larger networks is 10% better. This architecture is compatible with foundry designs and can be readily implemented into other neuromorphic architectures.

ACKNOWLEDGMENT

The authors acknowledge helpful discussions with A. Ne. This work has received funding from the European Union's Horizon 2020 research and innovation programme under Grant Agreement 780848 (Fun-COMP project), Grant Number 101017237 (PHOENICS project) and, more recently, European Union's Innovation Council Pathfinder programme under Grant Agreement No 101046878 (HYBRAIN project). This research was also supported via the Engineering and Physical Sciences Research Council Grants EP/J018694/1, EP/M015173/1, and EP/M015130/1 and a Clarendon Scholarship.

REFERENCES

- [1] C. Ríos et al. , *Sci Adv*, vol. 5, no. 2, p. eaa5759, Sep. 2022
- [2] J. Feldmann et al. , *Nature*, vol. 589, pp. 52–58, 2021
- [3] X. Li et al. , 2020 IEEE International Electron Devices Meeting (IEDM), Dec. 2020, pp. 7.5.1–7.5.4
- [4] H. Morino et al. , *Journal of Lightwave Technology*, vol. 32, no. 12, pp. 2188–2192, 2014
- [5] Q. Xu, et al. , *Opt. Express*, vol. 14, no. 20, pp. 9431–9436, Oct. 2006
- [6] A. Katumba, et al., *Sci Rep*, vol. 8, no. 1, p. 2653, 2018
- [7] W. M. Henry and J. D. Love, *Opt Quantum Electron*, vol. 29, no. 3, pp. 379–392, 19